Use of generalized population ratios to obtain Fe XV line intensities and linewidths at high electron densities

S. O. Kastner and A. K. Bhatia
Laboratory for Astronomy and Solar Physics, NASA-Goddard Space Flight Center, Greenbelt, Maryland 20771
(Received 1 February 1980)

A generalized method for obtaining individual level population ratios is used to obtain relative intensities of extreme ultraviolet Fe XV emission lines in the range 284–500 Å, which are density dependent for electron densities in the tokamak regime or higher. Four lines in particular are found to attain quite high intensities in the high-density limit. The same calculation provides inelastic contributions to linewidths. The method connects level populations and level widths through total probabilities t_{ij}, related to "taboo" probabilities of Markov chain theory. The t_{ij} are here evaluated for a real atomic system, being therefore of potential interest to random-walk theorists who have been limited to idealized systems characterized by simplified transition schemes.

INTRODUCTION

The spectroscopy of the magnesiumlike ion Fe XV is of potential importance in tokamak studies for purposes both of radiative energy loss determination and diagnostics of plasma temperature and density.[1] Recently[2] we have calculated the intensity ratios of extreme ultraviolet (euv) lines of Fe XV for a range of densities from $N_e = 10^6$–10^{12} cm^{-3}. In the present work the calculation is extended through current tokamak densities of about 10^{12}–10^{14} cm^{-3} to densities as high as 10^{21} cm^{-3} produced in laser-generated plasmas. Among results to be detailed below, it is shown that some lines of Fe XV reach higher intensities than the strong 284.15-Å resonance line. Density dependence of certain intercombination lines also appears for electron densities higher than 10^{12} cm^{-3}.

A novel feature of the present calculation is that instead of solving the full system of linear equations for statistical equilibrium—one for each level—as is usually done, a recent generalization of an expression for individual population ratios is used.[3] This method in principle will allow more efficient computation when not all population ratios of a given system are needed, especially for large systems, and is here shown to give the same results as in the standard method.

In carrying out the method, moreover, two further quantities of interest are obtained: (a) the collisionally induced width of each of the levels concerned, yielding the linewidths of associated spectral lines, additionally useful for plasma diagnostics and (b) the "total" transition probability between a given pair of levels, i.e., the probability t_{ij} that an electron leaving level i will arrive at level j before returning to i after traversing all possible paths through the levels of the system. The latter quantity is of some relevance for random-walk theory, which so far has dealt only with idealized systems having symmetric or simple asymmetric transition probabilities.[4] The present evaluation of t_{ij} for levels of Fe XV is believed to be the first such evaluation for a real system of atomic levels, and thus may be of interest to both atomic and statistical physicists.

METHOD

An explicit expression for the population ratio N_i/N_j in an n-level system was earlier given by Jefferies[5] as

$$\frac{N_i}{N_j} = \frac{\sum_k P_{jk} q_{ki,j}}{\sum_k P_{ik} q_{kj,i}}, \tag{1}$$

where P_{jk} is the transition rate from j to k and $q_{kj,i}$ is the probability that a transition from k to j occurs before a transition from k to i. Generalizations of this expression are given in Ref. 3, based on consideration of the level system as a Markov chain. An outline of the procedure follows.

The transition matrix P of an arbitrary system with states $1,2,3,\ldots,k,\ldots n$, of which one state k is absorbing, may be partitioned in the "canonical" form for a stochastic matrix:

$$P^k = \begin{bmatrix} 1 & 0 & 0 & \cdots & & & 0 \\ p_{2k} & 0 & p_{23} & \cdots & p_{21} & \cdots & p_{2n} \\ p_{3k} & p_{32} & 0 & \cdots & p_{31} & \cdots & p_{3n} \\ \cdot & & & & & & \\ \cdot & & & & & & \\ \cdot & & & & & & \\ p_{1k} & p_{12} & p_{12} & \cdots & 0 & \cdots & p_{1n} \\ \cdot & & & & & & \\ \cdot & & & & & & \\ \cdot & & & & & & \\ p_{nk} & p_{n2} & p_{n3} & \cdots & p_{n1} & \cdots & 0 \end{bmatrix} \equiv \begin{bmatrix} I & 0 \\ R & Q \end{bmatrix}, \tag{2}$$

i.e., the rows and columns corresponding to states 1 and k are interchanged, and submatrices Q^k and R^k are defined. In terms of these submatrices, further important matrices can be defined as $F^k = (1-Q^k)^{-1}$ and $B^k = F^k R^k$; B^k_{jk} is the probability that a random walker through the Markov chain will be absorbed in state k if it starts in state j.

With these definitions, it is shown in Ref. 3 that the total transition probability from i to j is $t_{ij} = B^j_{ij}/F^j_{ij}$, and further that the population ratio N_i/N_j of (1) is given equivalently by

$$\frac{N_i}{N_j} = \frac{T_j t_{ji}}{T_i t_{ij}} \equiv \frac{T_j B^i_{ji} F^j_{ji}}{T_i B^j_{ij} F^i_{jj}} , \tag{3}$$

where T_j is the total transition rate leaving state j.

It should be noted that throughout this description, the indices refer to states (levels) rather than rows and columns; in practice this difference affects only the matrix F and can be taken into account by substituting $F_{i-1,j}$ for $F_{i,j}$ throughout the calculation.

The calculation of the matrix $F = (I-Q)^{-1}$, termed the "fundamental matrix" in the literature, could be replaced if desired by calculation of a group generalized inverse matrix which is more economical to compute, according to work by Meyer[6] who shows that the latter matrix is easier to obtain. This alternative was, however, not utilized in the present first application of the method.

As mentioned in the Introduction, the quantities T_i and t_{ij} are obtained in the course of the calculation. Denoting actual collisional excitation (or deexcitation) rates by C_{ij} and spontaneous radiative transition rates by A_{ij}, the transition rates between levels i and j are

$$T_{ij} = \begin{cases} C_{ij} & (i<j) \\ C_{ij} + A_{ij} & (i>j) \\ 0 & (i=j) , \end{cases}$$

so that the (normalized) transition probability p_{ij}, an element of the transition matrix P, is given by

$$p_{ij} = T_{ij} \Big/ \sum_k T_{ik} \equiv T_{ij}/T_i ,$$

with $T_i \equiv \sum_k T_{ik}$. Thus T_i is the sum of all transition rates away from level i, both collisional and radiative, and is therefore just the (full) half-width of level i in frequency units (if rates are given in $\sec^{-1}$) when elastic contributions to the level widths can be neglected. The half-width of a spectral line between levels i and j is then $T_i + T_j$.

In the following sections we give line ratios of particular Fe XV lines as obtained by the present method, collisional-radiative damping widths of regular and metastable levels and resulting line-widths of resonance and subordinate lines, and examples of the total transition probabilities t_{ij}.

LINE INTENSITIES

Table I lists the 14 levels of Fe XV considered here. In the following text, transitions will be referred to by this level numbering. As described in Ref. 2, transition rates A_{ij} between these levels were computed by the Superstructure program[7] and collisional excitation rates C_{ij} were obtained from the distorted-wave program package developed at University College, London.[8] These were used to construct the normalized transition probability matrix P from which specific submatrices Q^j and R^j are then obtained by row and column interchanges involving level j, where j is one of the initial levels in a desired intensity ratio

$$\frac{I(i \to p)}{I(j \to q)} = \frac{N_i}{N_j} \frac{A_{ip}}{A_{jq}} \frac{E_{ip}}{E_{jq}} . \tag{4}$$

Here E_{ip} is the energy difference between levels i and p.

A preliminary calculation at high density showed that the intensities of the transitions $3s3d\,^1D_2 \to 3s3p\,^1P_1$ at 243.78 Å; $3s3d\,^3D_3 \to 3s3p\,^3P_2$ at 233.85 Å; $3s3d\,^3D_2 \to 3s3p\,^3P_1$ at 227.21 Å, and $3p^2\,^3P_2 \to 3s3p\,^3P_2$, newly identified at 304.85 Å in Ref. 2, reach values equal to or greater than the strong resonance line at 284.15 Å for densities $N_e > 10^{19}$ cm^{-3}. The relative intensities of these four lines should thus be particularly useful for investigation of laser-produced plasmas or dense fusion plasmas, and were computed over the density range 10^{13}–10^{21} cm^{-3} as shown in Fig. 1 (the intensity values of the line 227.21 Å are not included in the figure, to retain clarity, being simi-

TABLE I. Energy levels of Fe XV.

	Level		Calculated energy (Ry)	Observed energy (Ry)
1	$3s^2$	$^1S_0$	0	0
2	$3s3p$	$^3P_0$	2.116	2.132
3		$^3P_1$	2.169	2.184
4		$^3P_2$	2.293	2.313
5		$^1P_1$	3.240	3.207
6	$3p^2$	$^3P_0$	5.060	5.053
7		$^1D_2$	5.094	5.100
8		$^3P_1$	5.148	5.145
9		$^3P_2$	5.298	5.301
10		$^1S_0$	6.053	(6.012) [a]
11	$3s3d$	$^3D_1$	6.218	6.186
12		$^3D_2$	6.229	6.195
13		$^3D_3$	6.247	6.209
14		$^1D_2$	7.032	6.945

[a] Predicted value; see Ref. 2.

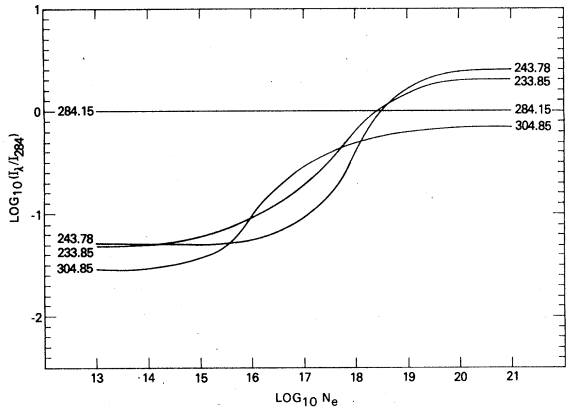

FIG. 1. Density dependence of the intensities of particular Fe XV lines, plotted relative to the intensity of 284.15 Å, which show marked increase at high densities.

lar to those of the line 304.85 Å). The leveling-off of intensities in Fig. 1 [and in following Fig. 2(a)] at high densities represents the expected approach to thermal equilibrium in which levels are Boltzmann populated.

Recently, Isler[9] noted Fe XV-like temporal behavior of a prominent line in the vicinity of 244 Å in a tokamak plasma, evidently the line 243.78 Å. It would be of interest to obtain independent electron-density measurements to verify the intensity variation predicted here for this line and the other three strong lines.

The same relatively high intensities should be attained at higher densities by the corresponding lines in the similar magnesiumlike ion Ni XVII; nickel is also used as a liner material in tokamaks. The Ni XVII lines, not yet observed, are predicted in Ref. 2 to be at the following wavelengths: 216.37 ± 0.25, 207.7 ± 0.5, 200.3 ± 0.5, and 267.0 ± 0.6 Å.

Lines at 307.75 (8 → 3) and at 312.55 Å (7 → 3) in the spectral neighborhood of the resonance line were also considered, of which 312.55 Å is an intercombination line. Another intercombination line of interest is 417.25 Å (3 → 1), which can be compared with the line 481.5 Å (7 → 5). The calculation was carried out for these lines with the resulting intensities shown in Fig. 2(a), relative to the resonance line. In Fig. 2(b) the relative intensities of spectrally adjacent pairs of the lines are plotted. These line ratios are seen to be density dependent in the range $N_e = 10^{14}$–10^{18}, especially the longer-wavelength pair of lines which are, however, weaker. According to Fig. 2(a) the intensities of the lines 312.55 and 307.75 Å become appreciable at higher densities so that these lines may prove more useful for diagnostic purposes. The results do not change appreciably for trial

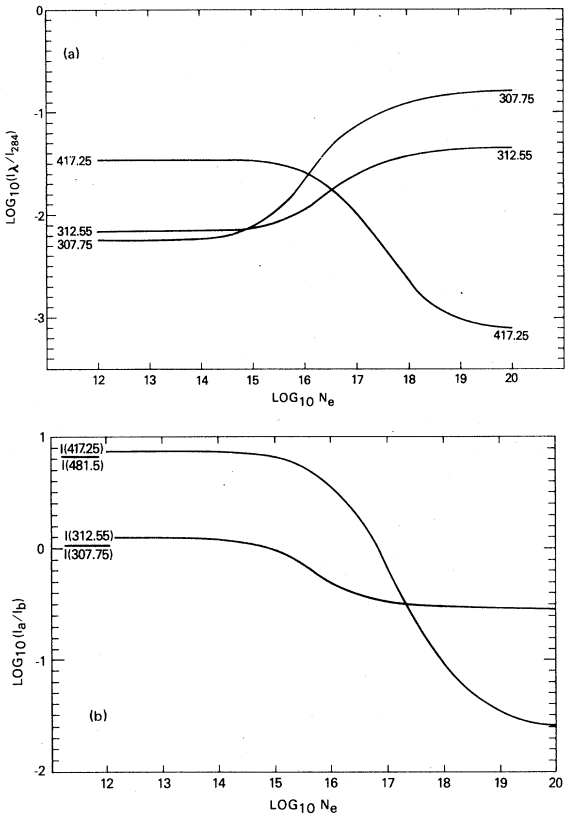

FIG. 2. (a) Relative intensities of other Fe XV lines, including intercombination lines, showing useful density dependence at intermediate densities. (b) Variation with density of the relative intensities of spectrally adjacent pairs of the lines in (a).

departures from the assumed temperature $T = 2.0 \times 10^6$ K, for which Fe XV has its maximum abundance.

To check line intensity ratios obtained by the present method against values calculated in Ref. 2 by the usual linear system solution, a comparison was made for some additional lines at several density values. Table II shows typical values obtained by the two methods. It is seen that agreement is excellent, apart from a difference in values for the transition 8 → 3 at low densities. This difference must originate in the different numerical procedures used, possibly in cancellation of terms of small magnitude, since the same atomic parameters were used in both cases. At the present time, in fact, it is not possible to decide which method is the more accurate.

LINEWIDTHS

In the impact approximation, the (full-width-half-maximum) width of an isolated ion line between levels i and f (we neglect possible level de-

TABLE II. Comparison of line intensity ratios [a] obtained by linear system solution (LSS) and present generalized population ratio (GPR).

Line ratio [b]	$N_e=10^2$ cm^{-3} LSS	GPR	$N_e=10^6$ cm^{-3} LSS	GPR	$N_e=10^{12}$ cm^{-3} LSS	GPR	$N_e=10^{19}$ cm^{-3} LSS	GPR
(4−3)/(5−1)	1.087(−3)	1.159(−3)	1.087(−3)	1.159(−3)	1.199(−5)	1.199(−5)	9.330(−11)	9.330(−11)
(3−1)/(5−1)	3.671(−2)	3.668(−2)	3.671(−2)	3.668(−2)	3.440(−2)	3.440(−2)	9.636(−4)	9.636(−4)
(8−3)/(5−1)	7.656(−6)	5.644(−4)	1.171(−5)	5.649(−4)	5.791(−3)	5.792(−3)	1.537(−1)	1.537(−1)
(7−3)/(5−1)	5.644(−3)	5.649(−3)	5.644(−3)	5.649(−3)	7.088(−3)	7.088(−3)	4.352(−2)	4.352(−2)
(12−4)/(5−1)	1.241(−3)	1.247(−3)	1.241(−3)	1.247(−3)	3.105(−3)	3.105(−3)	2.562(−1)	2.562(−1)
(13−4)/(5−1)	7.403(−3)	7.436(−3)	7.407(−3)	7.440(−3)	4.899(−2)	4.900(−2)	1.461(−0)	1.461(−0)

[a] Signs and integers in parentheses following significant figures represent powers of 10.
[b] Levels keyed to Table I.

generacies which may occur at the highest densities as a result of quasistatic Stark broadening) due to incident electrons of velocity v is given in angular frequency units by[10]

$$w=N_e\int_0^\infty f(v)v\left(\sum_{i'}\sigma_{i,i'}+\sum_{f'}\sigma_{f,f'}+\int|\phi_i-\phi_f|^2d\Omega\right)dv\,, \qquad (5)$$

where i',f' are levels to which i and f can, respectively, be excited (or deexcited), $\sigma_{i,j}$ are inelastic cross sections, and the ϕ_j are elastic scattering amplitudes for the states i, f, integration being carried out over the scattering angle Ω. The velocity average is taken over the Maxwellian distribution $f(v)$.

In the present highly ionized case where T is of the order 2×10^6 K, $kT\simeq 90$ eV is always greater than the separations ΔE between levels i and nearby perturbing levels i', or between f and nearby levels f', which are of the order of 25 eV or less. Incident energies are therefore well above all thresholds ΔE so that the term representing elastic contributions in (5) can probably be neglected. (In this respect a highly ionized ion appears to resemble the neutral atom case, for which also $kT>E$, rather than low stages of ionization for which the converse holds.[11]) The inelastic terms of (5) are just our computed total exit rates T_i and T_j less the spontaneous emission contributions which are included in T_i and T_f, i.e.,

$$w=T_i+T_f-\left(\sum_j A_{ij}+\sum_k A_{fk}\right). \qquad (6)$$

Instead of working with w as is usually done, for convenience we will define the full damping width $w_d=T_i+T_f$ which thus includes natural broadening; this w_d will not be a linear function of electron density at low values of N_e, of course, due to the independence of the A's.

The individual widths $w_d(i)=T_i$ and $w_d(f)=T_f$ of levels i and f, which are the actual level widths in the rest frame of the atom due to combined collisional and natural broadening, are not usually separately displayed but are felt to be of interest in themselves and therefore are plotted as a function of density in Fig. 3. The widths $w_d(1,2,4)$ are seen to be strictly proportional to N_e, being essentially completely collisional, whereas levels 3, 7, and higher have successively larger radiative contributions which give constant residual widths at low density. $w_d(2,4)$ are actually slightly less than $w_d(1)$, the ground level width; this would appear to be a general property of metastable levels such as 2 and 4. As one consequence, the rest-frame width of the visible forbidden transition 4 → 3 (7059 Å) is mainly due to the lower level 3, an interesting but not practically significant feature

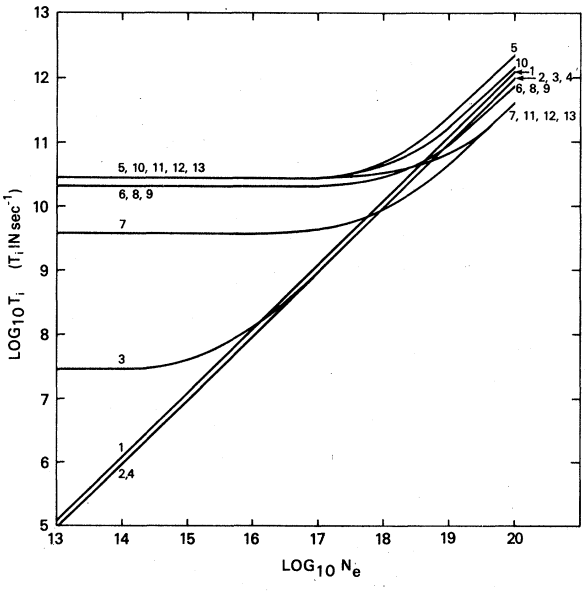

FIG. 3. Collisional-radiative damping widths $T_i\equiv w_d(i)$ of Fe XV levels (numbered according to Table I).

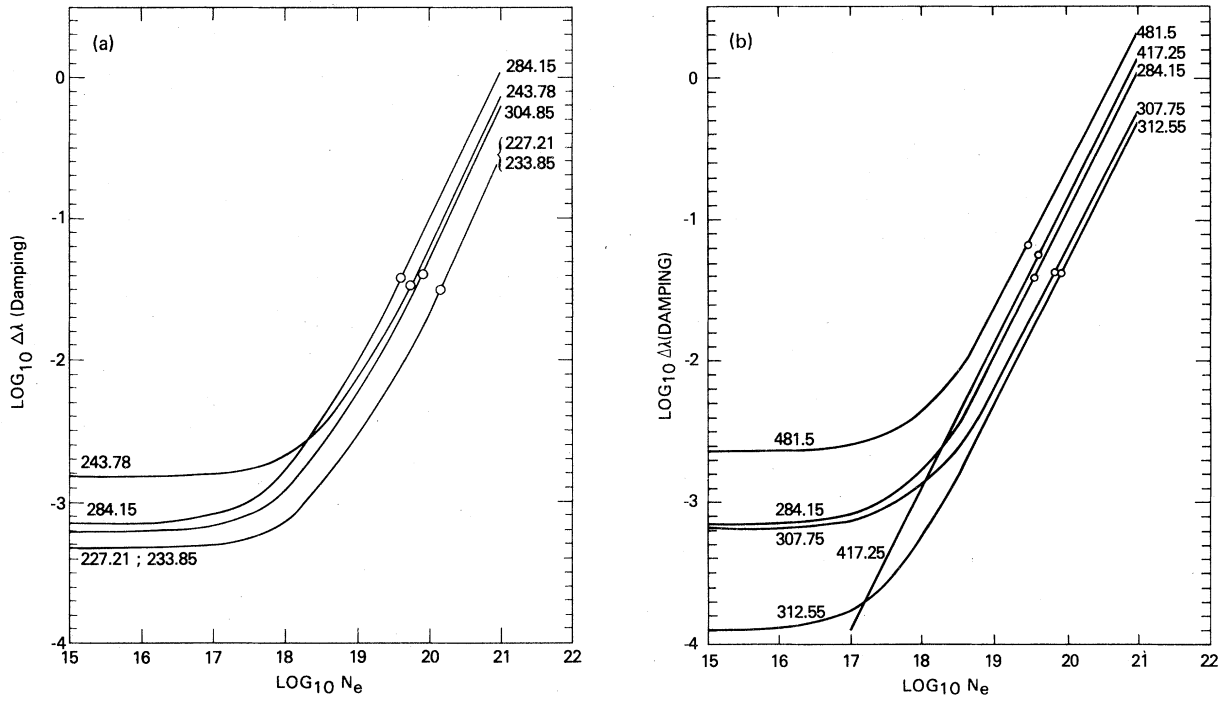

FIG. 4. (a) Damping linewidths of the stronger Fexv lines; open circles denote respective Doppler widths. (b) Damping linewidths of other density-sensitive Fexv lines; open circles again denote corresponding Doppler widths.

since Doppler broadening predominates at low densities. At high densities, it can be seen that the level widths become ordered in relative magnitude of collisional coupling, i.e., level 5 ($3s3p\ ^1P_1$) has the largest collisional rates to other levels, while levels 7 ($3p^2\ ^1D_2$) and 11, 12, and 13 ($3s3d\ ^3D_J$) have the lowest rates. As noted in connection with the line intensities the collisional rates and therefore the widths w_d are relatively insensitive to change in temperature.

TABLE III. Damping linewidths $\Delta_d\lambda$ and total linewidths $\Delta_T\lambda$ (Å). [a]

Line (Å)	$\log_{10}N_e$ 17	18	19	20	21	22
284.15	8.04(−4)	1.65(−3)	1.01(−2)	9.45(−2)	9.38(−1)	9.37(−0)
	3.92(−2)	3.96(−2)	4.42(−2)	1.08(−1)	9.40(−1)	9.37(−0)
243.78	1.60(−3)	2.15(−3)	7.64(−3)	6.25(−2)	6.11(−1)	6.10(−0)
	3.41(−2)	3.44(−2)	3.73(−2)	7.69(−2)	6.13(−1)	6.10(−0)
233.85	4.99(−4)	7.31(−4)	3.05(−3)	2.62(−2)	2.58(−1)	2.58(−0)
	3.22(−2)	3.23(−2)	3.35(−2)	4.76(−2)	2.62(−1)	2.58(−0)
304.85	6.82(−4)	1.17(−3)	6.07(−3)	5.51(−2)	5.45(−1)	5.45(−0)
	4.20(−2)	4.22(−2)	4.48(−2)	7.75(−2)	5.48(−1)	5.45(−0)
227.21	4.97(−4)	7.18(−4)	2.92(−3)	2.50(−2)	2.46(−1)	2.45(−0)
	3.13(−2)	3.14(−2)	3.35(−2)	4.59(−2)	2.49(−1)	2.45(−0)
307.75	7.37(−4)	1.25(−3)	6.41(−3)	5.80(−2)	5.74(−1)	5.73(−0)
	4.24(−2)	4.27(−2)	4.54(−2)	8.01(−2)	5.77(−1)	5.73(−0)
312.55	1.75(−4)	6.02(−4)	4.88(−3)	4.88(−2)	4.76(−1)	4.75(−0)
	4.27(−2)	4.29(−2)	4.52(−2)	7.35(−2)	4.80(−1)	4.75(−0)
417.25	1.34(−4)	1.33(−3)	1.33(−2)	1.33(−1)	1.33(−0)	1.33(+1)
	5.70(−2)	5.76(−2)	6.40(−2)	1.54(−1)	1.33(−0)	1.33(+1)
481.5	2.54(−3)	4.39(−3)	2.29(−2)	2.08(−1)	2.06(−0)	2.05(+1)
	6.69(−2)	6.80(−2)	7.82(−2)	2.27(−1)	2.06(−0)	2.05(+1)

[a] First-row entries are $\Delta_d\lambda$, second row entries are $\Delta_T\lambda$; signs and integers following significant figures represent powers of 10.

The damping linewidths $\Delta_d\lambda$ in wavelength units (Å) are plotted in Fig. 4(a) for the four strong lines discussed in the preceding section and in Fig. 4(b) for the other, weaker lines. The corresponding Doppler widths are included as open circles to show that the damping linewidths begin to contribute appreciably to the total linewidths for electron densities above 10^{17} cm^{-3}.

Table III gives values of the damping linewidth $\Delta_d\lambda$ (plotted in Fig. 4) and the total linewidth $\Delta_T\lambda$ which includes Doppler width at $T=2\times10^6$ K. The widths of the stronger lines will, of course, be most easily measurable. Again, it would be of much interest to compare experimentally measured widths with the currently calculated values, both to verify the theoretical assumptions and to enable the linewidths to be used for diagnostic work.

Before concluding this section some comments should be made. The collisionally induced linewidth values obtained here represent lower limits since the following sources of broadening have not been included: ion broadening of both quasistatic and impact character, depending on the plasma composition, and inelastic excitations to still higher levels, including ionization to the continuum; the latter contribution may be of importance when $kT > \Delta E$ as in the present case, but does not yet seem to have been considered in the context of line broadening.

Quantum-mechanical linewidth calculations have been carried out for singly charged ions by Bely and Griem[12] and by Barnes.[13] For such ions, as mentioned above, $kT \lesssim E$ so that elastic terms must be taken into account. It appears that highly charged ions may be simpler to deal with if excitation to higher levels and the continuum should be found to be not an important factor, but this remains to be investigated.

THE PROBABILITIES t_{ij}

The quantities t_{ij} appear to be related to the "taboo probabilities" of classical Markov chain theory, originally developed by Chung[14] and others and summarized, e.g., by Feller.[15] These are

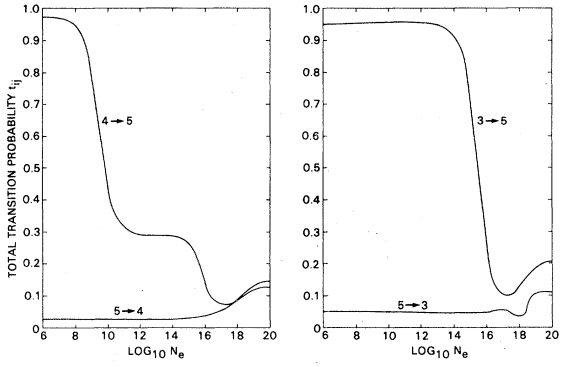

FIG. 5. Examples of the density dependence of total transition probabilities t_{ij}; numbers refer to the levels of Table I.

transition probabilities involving three states r,j,k of the system such that one of the states is avoided or "taboo" during the transition. In particular (using Feller's notation), if ${}_rp_{jk}^{(n)}$ is the probability of a transition on the nth step from j to k without intermediate passage through r, then the sum

$$ {}_r\pi_{jk}=\sum_{n=0}^{\infty} {}_rp_{jk}^{(n)} \tag{7}$$

is the total probability of transition from j to k without passage through r.

A particular result associated with this quantity which is of present interest is that

$$ \frac{{}_j\pi_{ii}}{{}_i\pi_{jj}}=\frac{u_i}{u_j}\,, \tag{8}$$

where u_i, u_j are the steady-state (invariant) occupation probabilities of states i and j; i.e., $\{u_k\}$ is the steady-state distribution of the Markov chain in question. Since $u_i/u_j=N_i/N_j$, the physical population ratio, it is evident that the quantities t_{ij} and ${}_j\pi_{ii}$ are closely related. In later work it is hoped that the exact correspondence will be clarified, which must be done with caution since the concepts involved are not straightforward, at the same time reconciling the various notations used by workers in different fields. The complex variation of the t_{ij}'s with electron density is illustrated in Fig. 5 for the level pairs (4,5) and (3,5).

[1]W. L. Wiese and S. M. Younger, in *Beam-Foil Spectroscopy*, edited by I. A. Sellin and D. J. Pegg (Plenum, New York, 1976), Vol. 2.
[2]A. K. Bhatia and S. O. Kastner, Sol. Phys. 65, 181 (1980).
[3]S. O. Kastner, Astrophys. Space Sci. 68, 245 (1980).
[4]K. Lakatos-Lindenberg and K. E. Shuler, J. Math. Phys. 12, 633 (1971).
[5]J. T. Jefferies, Astrophys. J. 132, 775 (1960).
[6]C. D. Meyer, SIAM (Soc. Ind. Appl. Math.) Rev. 17, 443 (1975).
[7]W. Eissner, M. Jones, and H. Nussbaumer, Comput. Phys. Commun. 8, 270 (1972).
[8]W. Eissner and M. J. Seaton, J. Phys. B 5, 2187 (1972).
[9]R. C. Isler, in the Symposium on Atomic Spectroscopy, Tucson, Arizona, 1979 (unpublished).
[10]M. Baranger, Phys. Rev. 112, 855 (1958).
[11]H. Griem, *Spectral Line Broadening by Plasmas* (Aca-

demic, New York, 1974).
[12]O. Bely and H. Griem, Phys. Rev. A 1, 97 (1970).
[13]K. S. Barnes, J. Phys. B 4, 1377 (1971).
[14]K. L. Chung, *Markov Chains with Stationary Transition Probabilities* (Springer, Berlin, 1960).
[15]W. Feller, *An Introduction to Probability Theory and Its Applications* (Wiley, New York, 1968).